

This work was written as part of one of the author's official duties as an Employee of the United States Government and is therefore a work of the United States Government. In accordance with 17 U.S.C. 105, no copyright protection is available for such works under U.S. Law.

Public Domain Mark 1.0

<https://creativecommons.org/publicdomain/mark/1.0/>

Access to this work was provided by the University of Maryland, Baltimore County (UMBC) ScholarWorks@UMBC digital repository on the Maryland Shared Open Access (MD-SOAR) platform.

**Please provide feedback**

Please support the ScholarWorks@UMBC repository by emailing [scholarworks-group@umbc.edu](mailto:scholarworks-group@umbc.edu) and telling us what having access to this work means to you and why it's important to you. Thank you.

## Impacts of an accumulation hiatus on the physical properties of firn at a low-accumulation polar site

Z. R. Courville,<sup>1,2</sup> M. R. Albert,<sup>2</sup> M. A. Fahnestock,<sup>3</sup> L. M. Cathles IV,<sup>4</sup> and C. A. Shuman<sup>5</sup>

Received 27 October 2005; revised 31 August 2006; accepted 11 December 2006; published 8 June 2007.

[1] Recent field investigations of a megadune region of East Antarctica provide evidence that differences in grain size, thermal conductivity, and permeability across a megadune profile are due to spatial accumulation variability in the absence of significant microclimate variations. The megadunes are low-amplitude (2–8 m), long-wavelength (2–5 km) bands with perceptible but low accumulation (less than 40 mm water equivalent (weq)  $\text{yr}^{-1}$ ) and accumulation hiatus within several kilometers proximity, as determined by remote sensing, surface feature classification, and ground-penetrating radar profiling. Our hypothesis that accumulation rate impacts the extent of temperature gradient-driven metamorphic growth in low accumulation rate sites is supported by measurements of various firn physical properties. Relatively small differences in accumulation rate (less than 40 mm weq  $\text{yr}^{-1}$ ) result in large differences in physical properties, including grain size, thermal conductivity, and permeability, which are apparent in satellite-based microwave data from both passive and active sensors. The differences in physical snow structure between low-accumulation areas and accumulation hiatus areas in the near surface are sufficiently distinct that evidence of past accumulation hiatus should be observable in the physical and chemical properties of an ice core record.

**Citation:** Courville, Z. R., M. R. Albert, M. A. Fahnestock, L. M. Cathles IV, and C. A. Shuman (2007), Impacts of an accumulation hiatus on the physical properties of firn at a low-accumulation polar site, *J. Geophys. Res.*, 112, F02030, doi:10.1029/2005JF000429.

### 1. Introduction

[2] Polar snow and firn are sensitive indicators of local climate. The physical structure of snow and firn, including grain size, shape, and spatial distribution, influences the microwave sensor response [e.g., Mätzler and Huppi, 1989], the air–snow exchange processes involving atmospheric chemistry [e.g., Dominé and Shepson, 2002], and the chemical and physical content of the firn that becomes the ice core record [e.g., Alley *et al.*, 1993]. The purpose of this paper is to discuss the impact of extreme near-surface metamorphism resulting from accumulation hiatus on firn structure, the resulting effect on physical properties, such as permeability and thermal conductivity, and possible implications for ice core and microwave sensor interpretation. Results from field investigations in central Antarctica in

2002–2004 are presented. Our hypothesis is that spatial differences in metamorphism are dominated by accumulation rate variations with temperature and other microclimate variations having a lesser effect.

### 2. Background

[3] Antarctic megadunes are long-wavelength (2–5 km), low-amplitude (2–8 m) features clearly visible from airborne and space-borne platforms as alternating bright and dark bands in the visible and microwave wavelengths [Fahnestock *et al.*, 2000]. Megadunes cover up to 900,000  $\text{km}^2$  across central Antarctica. The largest megadune field is in the vicinity of the Vostok research station, which suggests that understanding megadune characteristics may be valuable in ice core interpretation. By comparing satellite imagery of the area spanning 34 years, Fahnestock *et al.* [2000] found that the megadune patterns appear to migrate upwind at approximately 10 to 20  $\text{m yr}^{-1}$ .

[4] Accumulation rate variations across small-scale dune forms have been studied both in sand [e.g., Bagnold, 1941; Fryberger *et al.*, 1979] and in snow [e.g., Black and Budd, 1964; Whillans, 1975; Pettre *et al.*, 1986; Liston *et al.*, 2000], showing that windblown particulates tend to accumulate in local concave areas or on the lee faces of dunes. However, subsurface imaging presented by Frezzotti *et al.* [2002] shows that this is not the case in a megadune field crossed by the Italian International Trans-Antarctic Scien-

<sup>1</sup>Thayer School of Engineering, Dartmouth College, Hanover, New Hampshire, USA.

<sup>2</sup>Cryospheric and Terrestrial Sciences Division, Cold Regions Research and Engineering Laboratory, Hanover, New Hampshire, USA.

<sup>3</sup>Institute for Study of Earth, Oceans, and Space, University of New Hampshire, Durham, New Hampshire, USA.

<sup>4</sup>Department of the Geophysical Sciences, University of Chicago, Chicago, Illinois, USA.

<sup>5</sup>Cryospheric Sciences Branch, NASA Goddard Space Flight Center, Greenbelt, Maryland, USA.

tific Expedition (ITASE) traverse. Their measurements from ground-penetrating radar (GPR) supported by surface elevation data using GPS show internal sedimentary structures indicating that snow accumulates on the windward face of the dune and that the lee faces and troughs of the dunes experience little to no accumulation. These zones of little to no accumulation are defined here as accumulation hiatus zones. The varying accumulation modes cause the surface topography, primarily the dune face, to migrate slowly in the direction of the persistent katabatic winds. The leeward face of the dune, the region of accumulation hiatus, is slowly buried over time by accumulation on the windward face and its consequent upwind migration. The back slope is progressively ablated or “polished” by the katabatic winds. This type of enhanced accumulation on the upstream face and resulting propagation up current has been identified on the deep seafloor for low aspect ratio mud wave formation from sediment redistribution in steady currents [Flood, 1988; Normark *et al.*, 1980]. The upstream migration of sediment waves or dunes is a general property of a class of sediment forms known as antidunes [Kennedy, 1963]. For Antarctic megadunes, Frezzotti *et al.* [2002, 2005] conclude that the progressive movement of the dunes over a given location creates a periodic record that is not representative of regional or broader-scale climate phenomena. The windward faces of the dunes can have accumulation rates ranging from an estimated 20 to 30 mm weq yr<sup>-1</sup>, while the leeward faces have accumulation rates ranging from an estimated 0 to 5 mm weq yr<sup>-1</sup> [Frezzotti *et al.*, 2002].

[5] The leeward faces of the dunes exhibit a glaze surface during late winter months [Albert *et al.*, 2004]. This glaze surface is made up of two monograin ice crusts sandwiching a 1.5-cm-thick layer of vertically oriented recrystallized grains, as observed by earlier field work [Albert *et al.*, 2004] and at other hiatus sites [Fujii and Kusunoki, 1982]. The glazed region is easily recognized by its highly reflective surface when looking into the solar zenith. If buried, the glaze surfaces are preserved at depth as monograin ice crusts, as observed in previous studies of accumulation hiatus areas [Gow, 1968; Fujii and Kusunoki, 1982]. The top 2 m of the firn on the leeward faces of the megadunes consist of unusually large, well-sintered, vertically oriented growth crystals, which resemble hard depth hoar as described by Akitaya [1974] and Marbouty [1980]. We postulate that extensive temperature gradient-driven metamorphic growth observed on the leeward face is a result of decades of vapor transport at low temperature [Albert *et al.*, 2004].

### 3. Methods

[6] Field measurements were made during the 2003–2004 austral summer on the East Antarctic Plateau at a field camp located at 80.78°S, 124.49°E in a megadune region identified in satellite imagery and by GPS profiling during the 2002–2003 austral summer. This megadune region is characterized by low average annual temperature (−49°C), low accumulation rate (less than 40 mm weq yr<sup>-1</sup>), and nearly constant katabatic wind direction and wind speed (6–12 m s<sup>-1</sup>). This paper reports on measurements at two sites 3.4 km apart along a GPS-mapped line perpendicular to the dune fronts (approximately parallel to the

wind direction), one on the windward face of the dune in an area of snow accumulation and redistribution, and the other in the accumulation hiatus region on the leeward side of the dune (Figure 1). The sites selected for intensive snow pit studies included low-accumulation and hiatus regions classified as such by surface features described by Fujiwara and Endo [1971], Wantanabe, [1978], and Goodwin [1990] and by GPR surveying of the area (T. Scambos, personal communication, 2003).

[7] Automated weather stations (AWS) were installed at each site to measure air temperatures at heights of 1 and 2.5 m, wind speeds at heights of 1 and 7 m, and firn temperatures at several depths to 10 m. Three-cup anemometers (R.M. Young), with a range of 0 to 50 m s<sup>-1</sup> and an accuracy of ±0.5 m s<sup>-1</sup>, were used to measure the 1-m wind speeds. Propeller-type anemometers (R.M. Young), with a range of 0–60 m s<sup>-1</sup> and an accuracy of ±0.3 m s<sup>-1</sup>, were used to measure the 7-m wind speeds. The temperatures were measured using resistance temperature detectors (Honeywell HEL-700 Series Platinum RTDs), which are accurate to ±0.8°C at −100°C and ±0.5°C at 0°C. Their triple point was determined in distilled water/distilled water ice, resulting in an absolute error of 0.1°C at 0°C.

[8] Two-meter snow pits at each location were sampled for density, permeability, thermal conductivity, microstructure, and grain size and type measurements. These snow pits were located approximately 10 m away from the AWS towers associated with them; the pits and their associated AWS were located in areas with the same surface conditions. The pits were excavated, and the upwind face of the pit was shaved flat for stratigraphic observation and sampling. The snow bulk density in the pits was measured at a resolution of 3 cm using a 100-cc box cutter and spring scale. Samples of snow and firn microstructure were preserved in the field using dimethyl phthalate as a pore filler, following the procedure of Perla [1982]. The microstructure samples were frozen in the field and shipped to the laboratory for later processing. In the lab, these sections were cut and microtomed, and the snow was allowed to sublime in a cold room for 2 days. The pits resulting from snow sublimation were filled with a black carbon-based powder and polished. The resulting sample was photographed with a digital camera, and the resulting digital image was converted into a binary image and despeckled. Image Processing Workbench (IPW), a digital image processing program, was used to calculate the grain-scale properties by statistical analysis of pixels representing grain (white) and pore (black) space [Shi *et al.*, 1993], with the computed intercept lengths used to determine the grain and pore sizes reported here.

[9] The snow permeability was determined using a custom-built permeameter [Albert *et al.*, 2000], which measures the air flow rate and corresponding pressure drop through a cylindrical snow sample. The permeameter design is based on the double-head design of Shimizu [1970], which minimizes edge effects between the sample holder wall and the snow sample. The permeameter was tested in the laboratory using glass beads and again in the field using a sample of porous foam with a known permeability. Ten measurements with different flow rates were made on each snow sample.

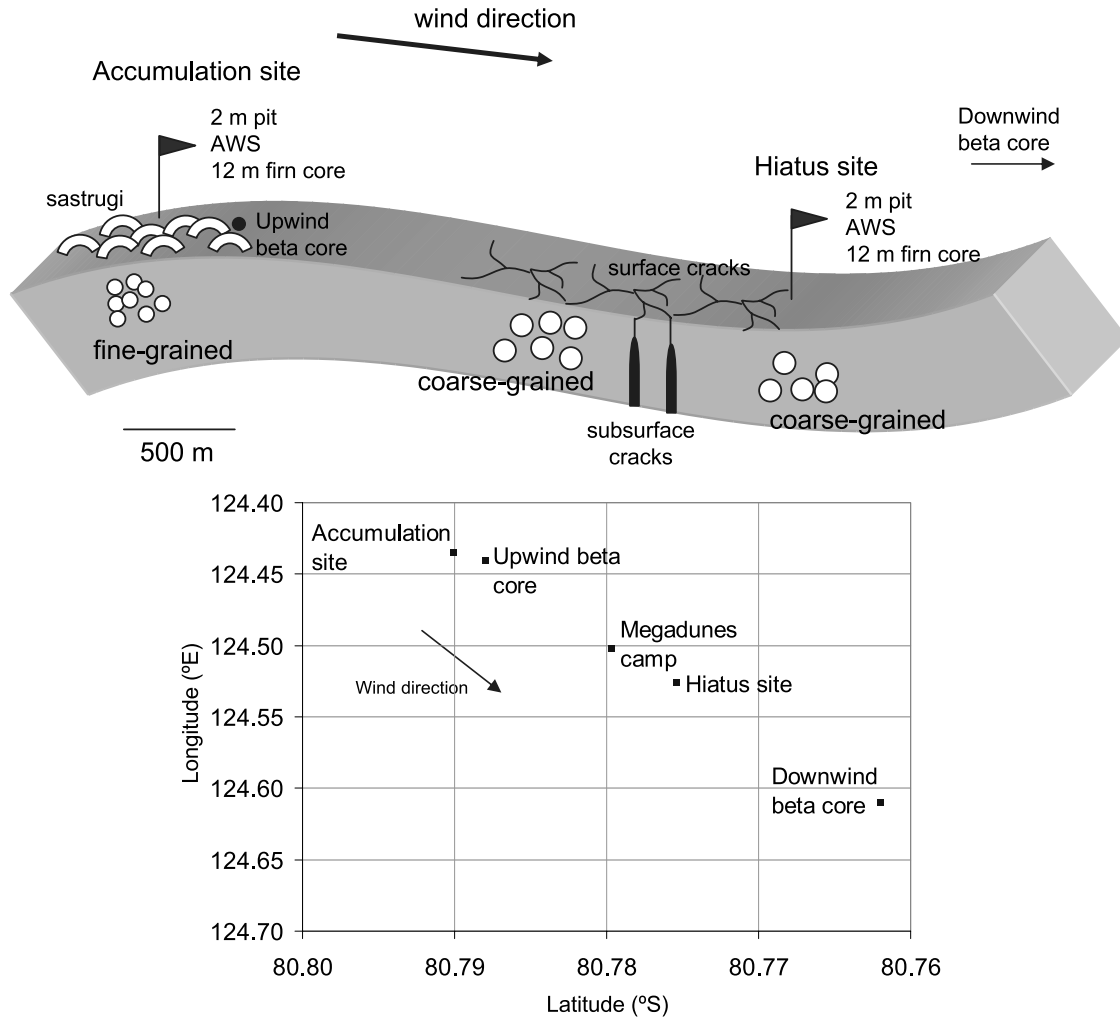


**Figure 1.** (top) Schematic of dune profile and sampling sites, (bottom) with an overhead latitude-longitude map of the area showing the measurement sites. Flags mark the position of 2-m snow pits and AWS towers. The accumulation site is approximately 3.4 km from the hiatus site.

Only the measurement pairs falling within the linear range were used to calculate permeability from Darcy's law:

$$v = -\frac{k}{\mu} \frac{dP}{dz}, \quad (1)$$

where  $v$  is the flow velocity,  $P$  is the pressure,  $\mu$  is the fluid viscosity,  $z$  is the sample height, and  $k$  is the permeability. The ten measurements were generally within 3% of one another. In previous field tests of the permeameter, different snow samples from the same depositional layer typically had permeability values that agreed to within 10%.

[10] The thermal conductivity was measured on firn cores in the laboratory using a needle probe that was inserted into the firn and heated. The heating curve of the probe was used to determine the thermal conductivity of the firn, a standard technique used in soils and as well as in snow [e.g., Lange, 1985; Sturm and Johnson, 1992]. The needle probe measured the effective thermal conductivity of the snow, which resulted from heat conduction through interconnected crystals plus the smaller latent and sensible heat transfer through the interstitial pore spaces. The firn core samples were

placed in a thick, close-fitting block of insulation with a thermal conductivity similar to firn in order to insulate the samples. The probe was allowed to equilibrate with the snow sample in the test assembly for 40 min before each thermal conductivity test was run. Temperature recordings from the probe showed that thermal equilibrium had been reached before each measurement. Replicate thermal conductivity measurements on the same snow sample are generally within 5% of one another.

[11] In addition to the snow pit samples, several shallow (2–12 m), hand-drilled firn cores were retrieved from each site 5 to 10 m from the pit locations and sent to the cold laboratory at the Cold Regions Research and Engineering Laboratory (CRREL) for further analysis. The permeability and density measurements as described above were repeated on 5- to 15-cm sections of the cores. When possible, layers of homogeneous grain size were preserved in single samples.

[12] Close to the two pit sites, two 8-m firn cores were retrieved from the crests of two sequential dunes and shipped to Woods Hole Oceanographic Institution for beta radioactivity measurements. The upwind beta core was drilled 250 m downwind from the accumulation snow pit

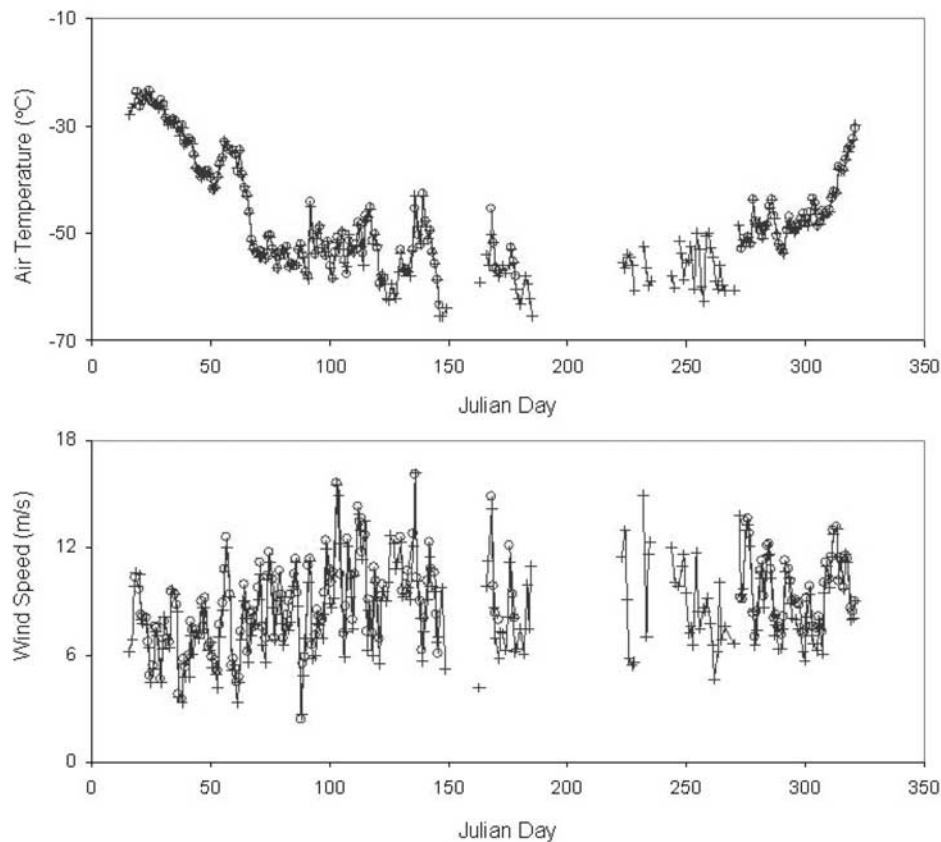


**Figure 2.** Comparison of hiatus site (circles) and accumulation site (pluses) (top) average daily air temperature at a height of 2.5 m and (bottom) wind speed at 7 m for the year 2004.

described below (Figure 1) on the crest of the dune. The downwind beta core was drilled on the subsequent dune crest, 4.2 km from the upwind core. In addition to the beta cores, GPR surveys were made on the line perpendicular to the dune fronts between the two cores in order to examine accumulation rate variations across the dune profile (T. Scambos, personal communication, 2003). GPR reveals isochronous surfaces in firn [e.g., *Hempel and Thyssen, 1992; Dahl-Jensen et al., 1997*]. The radar surveys show that the radioactive horizons fall along the same sedimentary horizon representing synchronous events. The detailed results from the GPR surveys, with discussion of the sedimentary structure of the dunes, will be presented in a future article (T. Scambos, personal communication, 2003).

#### 4. Measurements and Observations

[13] Both sets of beta radiation measurements are from areas of accumulation in this megadune region (dune crests) as opposed to the dune troughs and leeward faces. The 1965/66 beta radiation peaks in the cores occurred at depths of 376 and 464 cm, corresponding to accumulation rates of  $30 \pm 1$  and  $41 \pm 1$  mm weq yr<sup>-1</sup>, respectively (S. Das, personal communication, 2004).

[14] Hourly air temperature and wind speed data from the AWS towers over the course of one year are available. The daily averages over the course of the year are calculated from the hourly data. Comparisons of the average daily air temperature at a height of 2.5 m and average daily wind

speed at 7 m at the accumulation and at the hiatus site are shown in Figure 2. The gaps in the records are due to the AWS stations failing when the temperature was below  $-70^{\circ}\text{C}$ . For most of the year, the recorded daily air temperatures at the two sites differ by less than one degree. The average daily difference is  $0.2^{\circ}\text{C}$ , which could be attributed to instrumental calibration. The maximum difference over the year in the daily average recorded air temperature at 2.5 m is  $4.7^{\circ}\text{C}$  on Julian day 168. Such large temperature differences are infrequent, of short duration compared to the total record, and may be attributed to differential buildup of frost on the towers that can shield instruments from ambient conditions.

[15] For a period of several days immediately following the initial equipment set up in January 2004, data were collected every 15 or 20 min. We compared the synchronous wind speed and air temperature data from the two sites using a simple linear regression. The slope, intercept, and coefficient of determination ( $r^2$ ) between the synchronous temperatures and wind speeds of the accumulation site and the hiatus site at different heights are shown in Table 1 for average daily, hourly, and subhourly (15- to 20-min intervals) time frames. The two sites show nearly identical meteorological conditions.

[16] Following laboratory preparation, the thick section images of microstructure on the left-hand side of Figure 3 illustrate the difference in grain size between the accumulation and hiatus sites. The firn from the hiatus site is



**Table 1.** Results of Linear Fit of Hiatus Site Air Temperature and Wind Speed Data

	Wind Speed		Air Temperature	
	1 m	7 m	1 m	2.5 m
Slope				
Subhourly	0.847	0.896	0.996	0.996
Hourly	0.891	0.884	0.998	0.997
Daily	0.917	0.934	0.996	0.993
Intercept				
Subhourly	1.180	1.410	0.011	0.995
Hourly	0.970	1.580	0.091	−0.028
Daily	0.736	1.140	0.092	−0.012
$r^2$				
Subhourly	0.819	0.847	0.993	0.995
Hourly	0.835	0.847	0.990	0.993
Daily	0.934	0.947	0.994	0.995

composed of very large (larger than 0.5 mm in diameter) faceted grains of hard depth hoar, with an average grain diameter of 0.75 mm as determined by the digital image processing of the preserved microstructure. Crystals up to 1.5 cm in diameter were visually observed in the field using a hand lens. Previous researchers have made similar observations of large-crystal firn at other megadunes areas [Giovinetto, 1963; Gay *et al.*, 2002; Frezzotti *et al.*, 2002, 2005]. At the hiatus site, there was very little layering in the top 2 m of firn, as observed in pit stratigraphy. Grains from the accumulation site were much smaller than the hiatus grains, with an average grain diameter of 0.46 mm, and the

structure was best characterized as fine-grained wind pack, with small or fine grains defined as less than 0.2–0.5 mm, following Colbeck *et al.* [1990] and Gay *et al.* [2002]. The firn at the accumulation site also had many more visible stratigraphic layers in the top 2 m.

[17] The density measurements presented in Figure 3 show that the two sites have similar density profiles in the top 2 m. The corresponding permeability depth profiles from both sites are also presented in Figure 3. The thermal conductivity profiles measured on firn cores in the lab are presented in Figure 4, along with the density measurements of the same samples. Except for the top 30 cm, the thermal conductivity profile at the hiatus site is generally greater than at the accumulation site. The density profiles from the two sites are very similar.

## 5. Discussion

### 5.1. Characterizing Accumulation Regimes

[18] The windward faces of these megadunes are covered with wind-packed snow and are classified as an area of accumulation/redistribution characterized by small, 20- to 40-cm-high sastrugi, which are indicative of past deposition and current erosion and redistribution [Fujiwara and Endo, 1971]. The presence of multiple visible near-surface layers in GPR profiling also indicates that the windward face experiences net deposition (T. Scambos, personal communication, 2003), consistent with the results of the beta core, and more generally with observations of other megadune

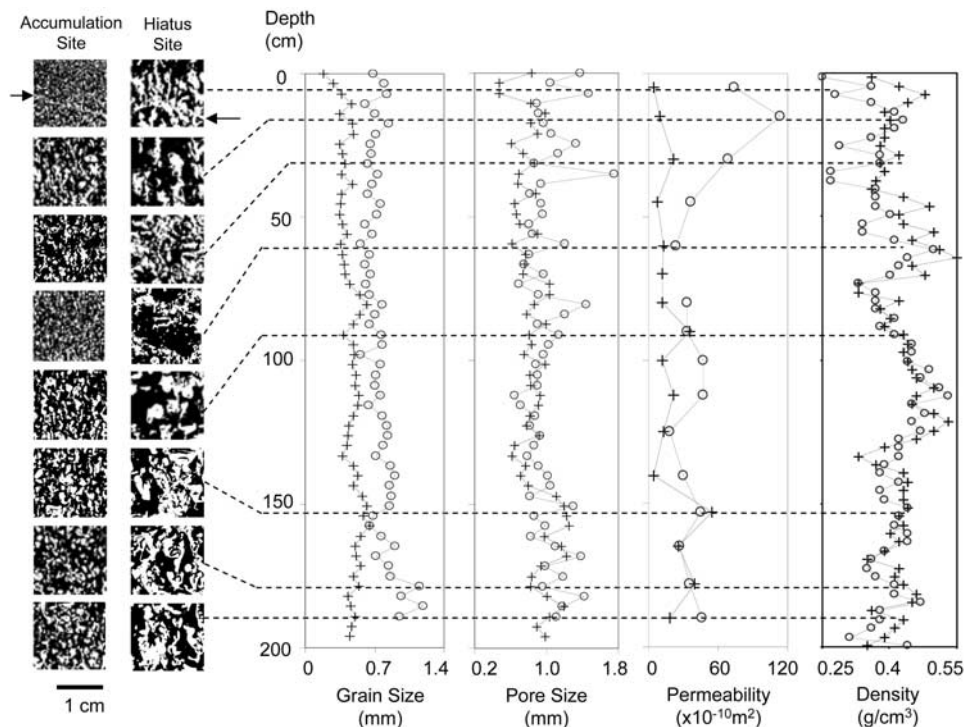


**Figure 3.** (left) Thick section images of firn microstructure at various depths from 2-m snow pits taken from an area of accumulation and an area of hiatus. Black represents pore space; white represents pits snow. The arrows point to ice crusts. (right) Graphs showing the corresponding variation of physical properties with depth. The open circles represent accumulation-hiatus firn; the plus signs represent accumulation firn.

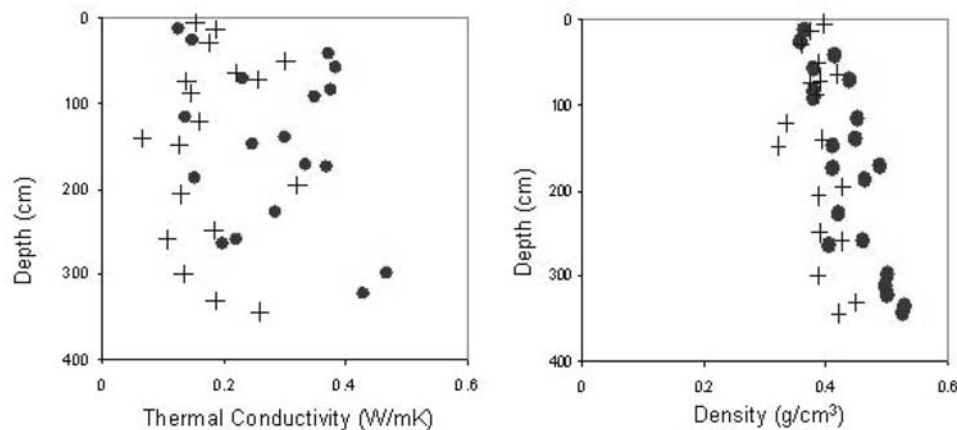


**Figure 4.** Thermal conductivity measurements made in the laboratory on core samples, with the corresponding density measurements for each sample. The plus signs represent measurements from the accumulation site; the solid circles represent the hiatus site.

areas by Frezzotti *et al.* [2002]. The accumulation rates measured at the dune crests are extremely low compared to rates reported across other areas of the Antarctic ice sheet, but are in the range of accumulation rates reported at a different megadunes area by Frezzotti *et al.* [2002].

[19] The leeward face of the dune is in an area of accumulation hiatus characterized by coarse-grained, vertically oriented, well-sintered firn. The field measurements reported here were conducted in January 2004, in the middle of the austral summer. The leeward surface was characterized by small ripple patterns, polygonal surface cracks, and was sastrugi free. The surface in this area was covered with a thin (1–2 cm) layer of recently deposited loose snow. Substantial snow redistribution and transport under clear-sky conditions was observed. The well-developed glaze surface that had been observed in November 2002, the late austral spring of the previous year [Albert *et al.*, 2004], was not visible on the surface but was observable at a depth of 1 to 2 cm in the leeward face snow pit. The observed glaze layer is indicative of a hiatus in accumulation [Gow, 1965; Wantanabe, 1978; Fujii and Kusunoki, 1982]. Below this glaze surface, the firn was composed of relatively homogeneous grains with little evidence of layering. One- to four-meter-thick zones of reduced reflection amplitude in GPR profiling also indicate that the leeward surface undergoes erosion or else little to no accumulation. (T. Scambos, personal communication, 2003).

## 5.2. Meteorological Conditions

[20] The wind speed data are similar for both sites on both subhourly and hourly timescales, as shown in Table 1. For the limited 15-min wind speed data at the two sites  $r^2 = 0.819$  at 1-m height and  $r^2 = 0.847$  at 7-m height. These  $r^2$  values are comparable to the hourly data at 1-m height ( $r^2 = 0.835$ ) and at 7-m height ( $r^2 = 0.847$ ) over the course of the year. Some of the variation between sites within the sub-hourly timescale can be attributed to the difficulty of obtaining synchronous observations at stations 3.4 km apart, i.e., there will be a time lag of approximately 5 min for one  $10 \text{ m s}^{-1}$  eddy to travel between the two sites. Assuming that there may also be small measurement errors

in absolute timing or velocity, it appears that, if there is a true difference in the wind speed between the sites, it is very small. Table 1 shows that the  $r^2$  value between the air temperature data from corresponding heights at the two sites are nearly identical, with  $r^2 = 0.993$  at 1-m height and  $r^2 = 0.995$  at 2.5-m height at 15-min intervals. These data show that both the accumulation site and the hiatus site experience very similar air temperature and wind speeds, even at relatively short timescales. Moreover, the 1-m temperature and wind speed measurements are within the undulation height of the megadunes. The dune amplitudes are about 5 m at this site, with dune wavelengths over 500 times greater than the amplitudes, based on GPS profiles across the area (T. Scambos, personal communication, 2003). This confirms that no wind or temperature shadowing effect occurs in the lee of the dunes. In other words, the air flow follows the topography.

[21] Steffen *et al.* [1999] reported on the formation of faceted crystals in a low-accumulation area ( $120 \text{ mm weq yr}^{-1}$ ) of northeast Greenland due to abrupt temperature changes caused by katabatic storms. The layers of faceted crystals were formed below wind crusts, as was observed at the megadunes. While the temperature data from the two megadunes sites do not indicate that the hiatus site experienced abrupt storm events while the accumulation site did not, the lack of snow accumulation at the hiatus site resulted the snow being exposed to growth-forcing temperature gradients on a longer timescale.

## 5.3. Firn Properties

[22] The observed differences in permeability between the accumulation and hiatus firn can be explained by variations in microstructure (Figure 3). The permeability is a reflection of the grain-scale nature of the firn and is sensitive to the geometry of the interconnected pore space [Albert *et al.*, 2004]. The constrictions, or “throats,” in the pore space contribute to the effective permeability of the firn. Grain size also influences the permeability, as smaller grains increase the drag in the airflow. The permeability of the surface snow at the hiatus site is much higher than that of the small-grained, tightly wind packed snow at the

accumulation site. The permeability of the surface snow at the hiatus site is lower than the hiatus firn at 20-cm depth because of the monograin ice crust at 1- to 2-cm depth (marked by the arrow in the microstructure image, Figure 3), which is the remnant of the previous season's surface glaze. The monograin ice crusts are less permeable than the large-grained, hiatus firn observed in the visual stratigraphy of the pit wall from 24- to 30-cm depth with no ice crusts, but these crusts are more permeable than the wind pack snow layers at the accumulation site. From 10 cm to approximately 30 cm, the permeability of the accumulation site firn increases, but is still much less permeable than the hiatus firn at the same depth. The permeability of the hiatus firn increases dramatically below approximately 10-cm depth as this portion of the firn contains no ice crusts. Below 30 cm, the firn at the accumulation site is generally less permeable than at the hiatus site. As noted above, at these depths, the snow grains and pore sizes are generally smaller at the accumulation site. While the permeability profile at any given site varies with depth because of layering, the hiatus site firn, with an average permeability of  $46 \times 10^{-10} \text{ m}^{-2}$  in the top 2 m, is significantly more permeable than the accumulation site firn, which has an average permeability of  $20 \times 10^{-10} \text{ m}^{-2}$  in the top 2 m. In general, the large, vertically oriented crystals developed via metamorphism appear to result in larger, vertically oriented interstitial pathways, which results in firn with a higher effective permeability.

[23] The crystal structure of the firn also impacts the thermal conductivity. At a given site, the thermal conductivity varies considerably between different layers, depending on the relative nature of the firn, i.e., whether it is fine- or coarse-grained firn relative to the firn at that site. At the accumulation site, the surface wind-packed layer, approximately the top 30 cm, has a slightly higher thermal conductivity than the hiatus surface firn because of its tightly packed, small, spherical grains (Figure 4). These grains have a high connectivity that allows the conduction of heat through several contact points to nearby neighboring grains. Below the top 30 cm, however, the firn at the hiatus site has a higher thermal conductivity because the larger, well-sintered snow grains conduct heat more readily through the grains as well as through the large intergranular bonds. In the top 4 m, the average thermal conductivities of the hiatus and accumulation sites are  $0.29 \text{ W m}^{-1} \text{ K}^{-1}$  with a standard deviation of  $0.11 \text{ W m}^{-1} \text{ K}^{-1}$  and  $0.19 \text{ W m}^{-1} \text{ K}^{-1}$  with a standard deviation of  $0.06 \text{ W m}^{-1} \text{ K}^{-1}$ , respectively. In ongoing work, we are using quantitative microscopy to examine the effect of microstructure geometry on the thermal conductivity of polar firn.

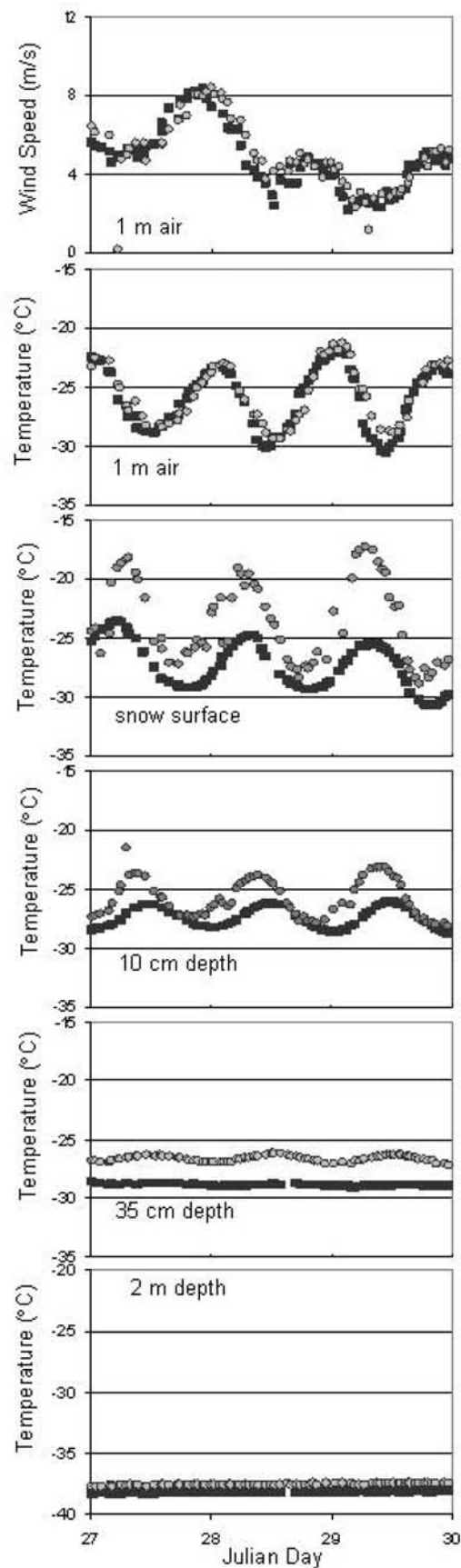
[24] In contrast to the permeability and thermal conductivity profiles, the density profiles of accumulation and hiatus areas are not significantly different from one another, as seen in Figure 3. The density profile from the hiatus site follows the same general trend as the profile from the accumulation site, most notably below 60 cm below the depth where the strong diurnal temperature gradients penetrate. Density-derived empirical formulae for permeability and thermal conductivity, which do not account for the effect of pore throat formation between large pore spaces on transport within the firn, will not predict these properties well at low accumulation rate sites. Therefore an approach

taking into account firn microstructure is necessary. Similarly, models for interpreting remotely sensed data commonly rely on density measurements and grain size, and there may be improvements which can be made by parameterization of the microstructural properties.

[25] The hourly temperatures at different depths in the firn are plotted for a period of 5 days in January when the temperature in the air was warmer than in the firn, the anemometers at both AWS towers were functioning, the thermistor string had stabilized after installation, and no significant accumulation had occurred to offset the thermistor depths (Figure 5). This data set demonstrates that temperature behaves as expected for a diffusion-dominated transport regime, with damping of temperature variations at depth. Although the accumulation and hiatus sites experience virtually the same air temperatures and wind speeds, the temperatures within the firn at corresponding depths show some systematic differences. The near-surface (top 10 cm) differences are likely due to a combination of the different thermal conductivity of the firn plus possible daytime solar heating of the thermistors. At deeper depths, the differences are primarily attributable to the different thermal conductivity profiles. The firn temperatures at the hiatus site are warmer in the top one meter than at corresponding depths at the accumulation site. The diurnal oscillations and the temperature difference between corresponding depths at the two sites decreases with depth, as expected. At 35-cm depth, the firn at the hiatus site is roughly  $3^\circ\text{C}$  warmer than at the accumulation site for this time in January. At 1-m depth, the difference is  $2.2^\circ\text{C}$ , and at 2-m depth, the difference is about  $0.5^\circ\text{C}$ . The amplitude of the diurnal variations in the temperature profile dies out faster at the accumulation site than at the hiatus site, and the phase difference between the subsurface temperatures and the air temperature increases with depth. If all of the diurnal variation in firn temperatures were due to solar heating of RTDs, the diurnal temperature oscillations in the firn would be in phase with those of the air temperature. However, because the phase lag between the firn temperature and air temperature increases with depth, there is evidence that the firn temperature differences are real, indicating that firn properties impact the temperature profiles.

[26] In polar regions, the temperatures in the top 20–30 cm of the firn are dominated by diurnal changes, while the temperatures between roughly thirty centimeters and several meters depth are dominated by weekly to seasonal variations in air temperature. At approximately 10-m depth the temperature remains fairly constant at approximately the average yearly air temperature. Our measurements of thermal conductivity and microstructure properties show that the thermal conductivity in the top 30 cm is slightly larger at the accumulation site, but between 30 cm and 4 m, the thermal conductivity at the hiatus site is generally much larger than at the accumulation site. The greater thermal conductivity of the firn below 30 cm at the hiatus site leads to deeper penetration of the diurnal air temperature oscillations than at the accumulation site. In addition, because most of the firn in the top several meters at the hiatus site has a higher thermal conductivity, the firn will be able to sustain less of a temperature gradient than that at the accumulation site. This is consistent with the measured temperature profiles in the top meters of the firn, which





are closer to the air temperature at the hiatus site than at comparable depths at the accumulation site.

[27] Our field measurements provide an explanation for the large differences in firn characteristics in this region. Over timescales ranging from 15 min to 1 day, the air temperatures and wind speeds at the accumulation and hiatus sites are very similar, with no differences of sufficient magnitude to have created the differences in firn properties that exist between the sites. At the hiatus site, while a light layer of recently deposited surface snow was observed in the middle of the relatively calm austral summer at the site, that same region had a surface glaze when visited in the windy late spring season [Albert *et al.*, 2004]. The near-surface stratigraphy observed at the hiatus site provides evidence that most of the loose midsummer snow was blown away by the higher winds of the winter and spring. Thus the primary difference between the accumulation and the hiatus sites is the difference in accumulation rate between the two sites. We therefore propose that the large difference in grain size between the two sites is due to the residence time of the snow crystals in the near-surface region as determined by the snow accumulation. The extensive temperature gradient–driven metamorphic growth caused by decades of vapor transport at the surface destroys the firn layering patterns in accumulation hiatus firn. A lower accumulation rate results in a longer residence time of a crystal in the top few centimeters of firn, where the temperature gradients that drive postdepositional metamorphism are the largest. By extension, at cold sites we predict that a vertical extent of large, homogeneous, well-bonded grains with high permeability and high thermal conductivity in a vertical section or ice core is evidence of an accumulation hiatus.

#### 5.4. Remote Sensing Signatures

[28] The field data can best be extrapolated across the region by the use of remote sensing data. Different accumulation rates result in different grain characteristics in the upper firn that impact both active and passive remote sensing data [e.g., Rotschky *et al.*, 2006]. Comparison of NSCAT measured backscatter on the Antarctic plateau [Long and Drinkwater, 1999] shows that high-backscatter areas correspond to the dune fields. Passive microwave sensors show low microwave emission for the same areas [Fahnestock *et al.*, 2000]. The high-backscatter signal is produced either by very rough surface conditions and distinct interfaces within the firn or by strong volume scattering from coarse grains, with diameter lengths on the same scale as the wavelength of the microwave signal.

**Figure 5.** Comparison of hourly temperatures at different depths in the firn at the accumulation and hiatus sites, along with wind speed and air temperature at 1 m. The hiatus firn temperatures are marked by the shaded circles, and the accumulation temperatures are marked by the solid squares. Note that though the thermistor strings were initially at the same approximate depths, both become buried over the course of the year. Because of the relatively low accumulation rate, this is not the major control on the observed differences. Also note the different scale on the bottom temperature plot at 2-m depth.

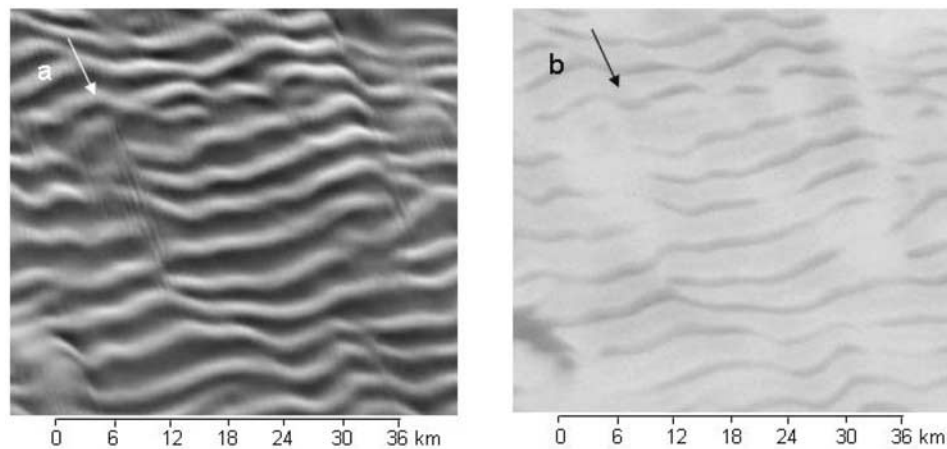


**Figure 6.** (a) MODIS visible-band image composite of megadune region studied. Illumination from the top right corner makes the upwind (accumulation) faces of the dunes appear bright. (b) Radarsat Antarctic mosaic of the same area. In this C band backscatter image the fine-grained upwind faces, which were bright in Figure 6a, are dark because of low energy return to the sensor. The overall bright signal is a result of the extensive temperature-gradient metamorphic growth of the low-accumulation areas discussed in the text. Note that the accumulation area occupies a small percentage of the total surface area. The arrows mark the general wind direction.

[29] In visible band MODIS (Moderate Resolution Imaging Spectroradiometer) images of megadune areas, the low surface relief becomes apparent (Figure 6a). The upwind faces, which represent areas of accumulation based on our field studies, appear bright in part due to the solar illumination angle at the time of image acquisition. In active C band Radarsat synthetic aperture radar (SAR) imagery of the same area, the megadunes' alternating bands of accumulation and hiatus appear as high and low backscatter intensity, respectively (Figure 6b). The accumulation bands, which are bright in the visible-band image, are dark in the radar image because of low energy return to the sensor. The overall bright signal of the Radarsat image in Figure 6b is due to the large spatial extent of extensively recrystallized grains from hiatus-type conditions. The dark bands representing accumulation areas cover only a small fraction of the image and overall area in the megadunes field. In megadunes areas, data from other sensors with a large footprint, such as passive microwave sensors, will be dominated by the firn characteristics of the hiatus areas of the region. Accordingly, in SSM/I data with an actual resolution of  $\sim 30\text{--}50$  km, the dune fields appear “cold” relative to other nearby areas in East Antarctica because of the extensive scattering of outgoing radiation in the more spatially extensive recrystallized firn in hiatus areas. Our field measurements show that in the accumulation hiatus regions, there are few internal layers in the top meters of firn, and the surface is unusually smooth; therefore the high radar backscatter in the accumulation hiatus area must be caused by the unusually large grain sizes.

[30] From our measurements, it is evident that microwave remote sensing data will be more sensitive to accumulation rate variations in low accumulation rate (less than  $40\text{ mm weq yr}^{-1}$ ) regions than in high accumulation rate regions. In cold, dry regions with accumulation rates larger than approximately  $150\text{ mm weq yr}^{-1}$ , such as are typical in

some parts of Antarctica, the surface firn gets buried before it can undergo significant metamorphism in the near-surface where large temperature gradients exist. For high-frequency sensors such as in the  $37\text{ GHz}$  range, the near-surface firn from an area with accumulation rate of  $300\text{ mm weq yr}^{-1}$  may not appear significantly different from an area where the accumulation rate is  $150\text{ mm weq yr}^{-1}$  because the residence time of snow crystals in the near-surface snow is short enough to limit postdepositional metamorphism.

## 6. Relevance to Ice Core Interpretation

[31] Ice cores drilled in polar regions provide a record of past climate conditions, both in the chemical composition and in the physical properties of the sampled ice. Our measurements show that an accumulation hiatus results in large crystals, little evidence of layering, and large permeability and thermal conductivity in near-surface firn relative to a nearby accumulation area. Postdepositional changes in physical, isotopic, and reactive species composition of the firn are sensitive to environmental conditions [e.g., Rick and Albert, 2004; Neumann and Waddington, 2004; Ekaykin *et al.*, 2002; Hutterli *et al.*, 2003]. Thus the existence of an accumulation hiatus will increase the likelihood of altered physical, chemical, and isotopic content of the near-surface firn. Our data indicate that an accumulation hiatus should be expressed in an ice core as a relatively thick, uniform layer not indicative of annual cycles, with evidence of more extensive postdepositional processing (grain growth from vapor transport and metamorphism) than surrounding layers.

## 7. Conclusions

[32] Near-surface firn at an accumulation hiatus site is characterized by significant (on the order of tens of centi-

meters and more) depths of large grained, well-sintered firn with higher permeability and higher thermal conductivity than at a nearby site experiencing the same microclimate but a slightly higher accumulation rate. At polar sites with accumulation rates less than approximately  $40 \text{ mm weq yr}^{-1}$ , accumulation rate has a first-order effect on firn microstructure, thermal conductivity, and permeability, with a smaller effect on density. Large spatial gradients in microwave signatures in megadunes areas are due to relatively small differences in accumulation rate (approximately  $40 \text{ mm weq yr}^{-1}$ ), while regions with high accumulation rates (e.g., higher than  $150 \text{ mm weq yr}^{-1}$ ) should not exhibit the same sensitivity to accumulation rate differences. The ice core record from an area of accumulation hiatus is expected to have a relatively thick, uniform layer of reduced internal layering due to years of temperature gradient-driven metamorphic growth in the near surface, likely to be accompanied by altered isotopic and reversibly deposited chemical species concentrations. The same temperature gradient-driven metamorphic growth process will result in very high backscatter and low microwave emission in accumulation hiatus areas.

[33] **Acknowledgments.** The authors would like to thank Ted Scambos for making his unpublished data available to support the discussion in this paper. There are several others whom we are indebted to in the collection of the data. Terry Haran (NSIDC) installed the AWS equipment used to collect the meteorological data. Rob Bauer (NSIDC) assisted Ted Scambos with the GPR effort as well as with our firn sample collection. The members of the Light Ground Traverse team helped set up the Megadunes camp. Tom Neumann and Dan Dixon collected surface cores as part of the traverse efforts. Sarah Das (WHOI) provided the beta core analyses. The 109th Air National Guard and Ken Borek Air provided superior air service in Antarctica. Raytheon Polar Services provided logistics and science support in Antarctica, and Ice Coring and Drilling Services provided coring devices and assistance. We would also like to acknowledge the helpful comments of several reviewers. This work was supported by the National Science Foundation (grant NSF-OPP 0125276).

## References

- Akitaya, E. (1974), *Studies on Depth Hoar*, Contrib. Inst. Low Temp. Sci., Ser. A, vol. 26, 67 pp., Hokkaido Univ., Sapporo, Japan.
- Albert, M. R., E. Shultz, and F. Perron (2000), Snow and firn permeability measurements at Siple Dome, Antarctica, *Ann. Glaciol.*, **31**, 353–356.
- Albert, M. R., C. Shuman, Z. Courville, R. Bauer, M. Fahnestock, and T. Scambos (2004), Extreme firn metamorphism: Impact of decades of vapor transport on near-surface firn at a low-accumulation glazed site on the East Antarctic Plateau, *Ann. Glaciol.*, **39**, 73–78.
- Alley, R. B., et al. (1993), Abrupt increase in Greenland snow accumulation at the end of the Younger Dryas event, *Nature*, **362**(6420), 527–529.
- Bagnold, R. A. (1941), *The Physics of Blown Sand and Desert Dunes*, CRC Press, Boca Raton, Fla.
- Black, H. P., and W. Budd (1964), Accumulation in the region of Wilkes, Wilkes Land, Antarctica, *J. Glaciol.*, **5**(37), 3–15.
- Colbeck, S. C., E. Akitaya, R. Armstrong, H. Gubler, J. Lafeuille, K. Lied, D. McClung, and E. Morris (1990), The international classification for seasonal snow on the ground, report, 21 pp., Int. Comm. on Snow and Ice, Int. Assoc. of Sci. Hydrol., Wallingford, U. K.
- Dahl-Jensen, D., N. S. Gundestrup, K. R. Keller, S. J. Johnsen, S. P. Gogineni, C. T. Allen, T. S. Chuah, H. Miller, S. Kipstuh, and E. D. Waddington (1997), A search in north Greenland for a new ice-core drill site, *J. Glaciol.*, **43**, 300–306.
- Dominé, F., and P. B. Shepson (2002), Air–snow interactions and atmospheric chemistry, *Science*, **297**, 1506–1510.
- Ekaykin, A. A., V. Y. Lipenkov, N. I. Barkov, J. R. Petit, and V. Masson-Delmotte (2002), Spatial and temporal variability in isotope composition of recent snow in the vicinity of Vostok station, Antarctica: Implications for ice core interpretation, *Ann. Glaciol.*, **35**, 181–186.
- Fahnestock, M. A., T. A. Scambos, C. A. Shuman, R. J. Arthern, D. P. Winebrenner, and R. Kwok (2000), Snow megadune fields on the Eastern Antarctic Plateau: Extreme atmosphere–ice interaction, *Geophys. Res. Lett.*, **27**(22), 3719–3722.
- Flood, R. D. (1988), A lee wave model for deep-sea mudwave activity, *Deep Sea Res.*, **35**(6), 973–983.
- Frezzotti, M., S. Gandolfi, and S. Urbini (2002), Snow megadunes in Antarctica: Sedimentary structure and genesis, *J. Geophys. Res.*, **107**(D18), 4344, doi:10.1029/2001JD000673.
- Frezzotti, M., et al. (2005), Spatial and temporal variability of snow accumulation in East Antarctica from traverse data, *J. Glaciol.*, **51**(172), 113–124.
- Fryberger, S., T. Ahlbrandt, and S. Andrews (1979), Origin, sedimentary features, and significance of low-angle aeolian sand sheet deposits, Great Sand Dunes National Monument and vicinity, Colorado, *J. Sediment. Petrol.*, **49**(3), 733–746.
- Fujii, Y., and K. Kusunoki (1982), The role of sublimation and condensation in the formation of ice sheet surfaces at Mizuho Station Antarctica, *J. Geophys. Res.*, **87**(C6), 4293–4300.
- Fujiwara, K., and Y. Endo (1971), Preliminary report of glaciological studies, in *Report of Japanese Traverse, Syowa-South Pole 1968–69*, edited by M. Murayama, *Jpn. Antarct. Res. Exped. Sci. Rep. Spec. Issue*, **2**, 68–109.
- Gay, M., M. Fily, C. Genthon, M. Frezzotti, H. Oerter, and J.-G. Winther (2002), Snow grain-size measurements in Antarctica, *J. Glaciol.*, **48**(163), 527–535.
- Giovinetto, M. B. (1963), Glaciological studies on the McMurdo–South Pole Traverse, 1960–1961, *Inst. Polar Stud. Rep.* **7**, Ohio State Univ., Columbus.
- Goodwin, I. (1990), Snow accumulation and surface topography in the katabatic zone of Eastern Wilkes Land, Antarctica, *Antarct. Sci.*, **2**(3), 235–242.
- Gow, A. J. (1965), Snow studies in Antarctica, *CRREL Res. Rep.* **177**, 19 pp., Cold Reg. Res. and Eng. Lab., Hanover, N. H.
- Gow, A. J. (1968), Deep core studies of the accumulation and densification of snow at Byrd Station and Little America V, Antarctica, *CRREL Res. Rep.* **197**, 44 pp., Cold Reg. Res. and Eng. Lab., Hanover, N. H.
- Hempel, L., and F. Thyssen (1992), Radio echo sounding of horizontal layers in ice, *J. Glaciol.*, **12**, 383–397.
- Hutterli, M. A., J. R. McConnell, R. C. Bales, and R. W. Stewart (2003), Sensitivity of hydrogen peroxide and formaldehyde preservation in snow to changing environmental conditions: Implications for ice cores, *J. Geophys. Res.*, **108**(D1), 4023, doi:10.1029/2002JD002528.
- Kennedy, J. F. (1963), The mechanics of dunes and antidunes in erodible-bed channels, *J. Fluid Mech.*, **16**, 521–544, doi:10.1017/S0022112063000975.
- Lange, M. A. (1985), Measurements of thermal parameters in Antarctic snow and firn, *Ann. Glaciol.*, **6**, 100–104.
- Liston, G. E., J. G. Winther, O. Bruland, H. Elvehoy, K. Sand, and L. Karlof (2000), Snow and blue-ice distribution patterns on the coastal Antarctic Ice Sheet, *Antarct. Sci.*, **12**(1), 69–79.
- Long, D., and M. Drinkwater (1999), Cryospheric applications of NSCAT data, *IEEE Trans. Geosci. Remote Sens.*, **37**(3), 1671–1684.
- Marbouty, D. (1980), An experimental study of temperature-gradient metamorphism, *J. Glaciol.*, **26**(94), 303–312.
- Mätzler, C. H., and R. Huppi (1989), Review of signature studies for microwave remote sensing of snowpacks, *Adv. Space Res.*, **9**(1), 253–265.
- Neumann, T. A., and E. D. Waddington (2004), Effects of firn ventilation on isotopic exchange, *J. Glaciol.*, **50**(169), 183–194.
- Normark, W. R., G. R. Hess, D. A. V. Stow, and A. J. Bowen (1980), Sediment waves on the Monterey fan levee: A preliminary physical interpretation, *J. Sediment. Res.*, **1**(70), 84–93.
- Perla, R. (1982), Preparation of section planes in snow specimens, *J. Glaciol.*, **28**(98), 199–204.
- Pette, P., J. F. Pinglot, M. Pourchet, and L. Reynaud (1986), Accumulation in Terre Adélie, Antarctica: Effect of meteorological parameters, *J. Glaciol.*, **32**, 486–500.
- Rick, U., and M. R. Albert (2004), Firn microstructure impacts on air permeability, *ERDC-CRREL Tech. Rep. TR-96*, 79 pp., Cold Reg. Res. and Eng. Lab., Hanover, N. H.
- Rotschky, G., W. Rack, W. Dierking, and H. Oeter (2006), Retrieving snowpack and accumulation estimates from a combination of SAR and scatterometer measurements, *IEEE Trans. Geosci. Remote Sens.*, **44**(4), 943–956.
- Shi, J., R. Davis, and J. Dozier (1993), Stereological determination of dry-snow parameters for discrete-scatterer microwave modeling, *Ann. Glaciol.*, **17**, 295–299.
- Shimizu, H. (1970), *Air Permeability of Deposited Snow*, Contrib. Inst. Low Temp. Sci., Ser. A, vol. 22, 32 pp., Hokkaido Univ., Sapporo, Japan.
- Steffen, K., W. Abdalati, and I. Sherjal (1999), Faceted crystal formation in the northeast Greenland low-accumulation region, *J. Glaciol.*, **45**(149), 63–68.
- Sturm, M., and J. B. Johnson (1992), Natural convection in the subarctic snow cover, *J. Geophys. Res.*, **96**(B7), 11,657–11,671.

Watanabe, O. (1978), Stratigraphic studies of the snow cover in Mizuho Plateau, *Mem. Natl. Inst. Polar Res. Spec. Iss. Jpn.*, 7, 154–181.

Whillans, I. M. (1975), Effect of inversion winds on topographic detail and mass balance on inland ice sheets, *J. Glaciol.*, 14(70), 85–90.

---

M. R. Albert and Z. R. Courville, Cryospheric and Terrestrial Sciences Division, Cold Regions Research and Engineering Laboratory, 72 Lyme Road, Hanover, NH 03755, USA. (zoe.courville@dartmouth.edu)

L. M. Cathles IV, Department of the Geophysical Sciences, University of Chicago, Chicago, IL 60637, USA.

M. A. Fahnestock, Institute for Study of Earth, Oceans, and Space, University of New Hampshire, Durham, NH 03824, USA.

C. A. Shuman, Cryospheric Sciences Branch, NASA Goddard Space Flight Center, Code 971, Greenbelt, MD 20771, USA.



Table 1. Results of Linear Fit of Hiatus Site Air Temperature and Wind Speed Data

	Wind Speed		Air Temperature	
	1 m	7 m	1 m	2.5 m
Slope				
Subhourly		0.847	0.896	0.996
Hourly	0.891		0.884	0.997
Daily	0.917		0.934	0.993
Intercept				
Subhourly		1.180	1.410	0.011
Hourly	0.970		1.580	-0.028
Daily	0.736		1.140	-0.012
r2				
Subhourly		0.819	0.847	0.993
Hourly	0.835		0.847	0.993
Daily	0.934		0.947	0.995